Journal of Catalysis **203,** 443–452 (2001)
doi:10.1006/jcat.2001.3326, available online at http://www.idealibrary.com on IDEAL®

Vanadium Oxide Supported on Mesoporous MCM-41 as Selective Catalysts in the Oxidative Dehydrogenation of Alkanes

B. Solsona, T. Blasco, J. M. López Nieto,[1] M. L. Peña, F. Rey, and A. Vidal-Moya

Instituto de Tecnología Química, UPV-CSIC, Avenida de los Naranjos s/n, 46022 Valencia, Spain

Received April 4, 2001; revised June 22, 2001; accepted July 2, 2001

The application of different techniques (^{51}V NMR, diffuse reflectance, and TPR-H_2) in the characterization of vanadia supported on mesoporous MCM-41 catalysts shows that the nature of the vanadium species depends on the V loading. In dehydrated catalysts with V content lower than 7 wt%, vanadium is mainly in a tetrahedral environment. In the presence of moisture, most V^{5+}, placed in accessible positions, binds to water molecules, becoming hexacoordinated, while some V^{5+} species, probably located within the pore walls, keep their tetrahedral coordination. Higher V contents in the catalyst leads to the formation of polymeric V_2O_5-like species. Both XRD and textural results indicate that the mesoporous structure of the support is mostly maintained after the vanadium incorporation, and therefore high surface areas were obtained on the final catalysts. MCM-41-suppported vanadia catalysts are active and selective in the oxidative dehydrogenation of propane and ethane, although the catalytic behavior depends on the V loading. A high rate of formation of propylene or ethylene per unit mass of catalyst per unit time have also been observed as a consequence of the high dispersion of V atoms achieved on the surface of the support. © 2001 Academic Press

Key Words: **supported vanadium oxide catalyst; siliceous mesoporous MCM-41; TPR; UV–Vis; ^{51}V NMR; oxidative dehydrogenation of propane and ethane; propylene or ethylene production.**

INTRODUCTION

The behavior of vanadium oxide supported on metal oxides (1–4) and vanadium substituted into molecular sieves (5–9) as catalysts in gas phase selective oxidation reactions is related to the nature of the V species. Moreover, the dispersion, the coordination, and the oxidation state of the V atoms depend not only on the V loading but also on the nature of the carrier employed for dispersing the vanadium atoms.

SiO_2-supported vanadia materials have been reported to be selective catalysts for the oxidative dehydrogenation, OXDH, of methanol (9, 10) and short-chain alkanes (11–13). Low V-loading catalysts are the most selective in the alkane oxydehydrogenation, but low productivities are generally obtained as a consequence of the low number of active sites. Therefore, one must use high surface area silica supports to obtain high conversions, keeping the selectivity at the desired level. In this line a new scope of high surface area materials was opened when the new family of siliceous mesostructured materials M41S was reported in 1991 by Mobil researchers (14). Among these solids, the most widely studied have been those with the MCM-41 structure, which possesses a regular hexagonal array of pores whose diameters can be easily tailored between 20 and 100 Å.

Interestingly, other atoms different from silicon can be incorporated into the mesoporous silica matrix, conferring to the final materials catalytic properties. This is the case of vanadium-substituted mesoporous molecular sieves, V–MCM-41 and V–MCM-48, which can be prepared by following a one-pot synthesis procedure (15–21). These materials show redox properties (18–20) and they have been recently reported as selective catalysts in the oxidative dehydrogenation of propane (19, 20) or in the selective oxidation of methanol to formaldehyde (18). In both reactions, the selectivities to oxydehydrogenation products on V-containing mesoporous materials are higher than those corresponding to silica-supported vanadia catalysts. However, these high selectivities when using mesoporous MCM as the support were usually obtained at low V contents, while a significant decrease of selectivity to propylene from propane occurs on catalysts with V contents higher than 1 wt% (19, 21).

An alternative method to incorporate vanadium onto silica surfaces is the use of grafting procedures (19, 22, 24, 25) or direct impregnation (22–24, 26) of the appropriate V-containing solutions on MCM materials. The resulting supported VO_x/MCM catalysts show redox properties similar to those obtained by one-pot synthesis procedures (19, 22, 24–26), but generally exhibit worse catalytic performance. Nevertheless, it is possible to obtain a relatively high space–time yield of formaldehyde during the selective oxidation of methane or methanol on VO_x/MCM-41 (25) and VO_x/MCM-48 (26), respectively. Also, high selectivities

[1] To whom correspondence should be addressed. Fax: 34-96-3877809. E-mail: jmlopez@itq.upv.es.

0021-9517/01 $35.00
Copyright © 2001 by Academic Press
All rights of reproduction in any form reserved.

to propylene during the oxidative dehydrogenation of propane on VO_x/MCM-48 have been reported (19). Although these systems have been scarcely studied, the preparation procedure appears to be crucial on the catalytic behavior of the resulting materials (19, 21, 25, 26).

The aim of this paper is to study the nature of V species formed on MCM-41-supported vanadia catalysts (VO_x/MCM-41) prepared by impregnation with an alcoholic solution. We shall compare the catalytic results in the oxidative dehydrogenation of propane and ethane over MCM-supported vanadia catalysts. We shall also show that MCM-based catalysts are active and selective in the oxydehydrogenation of short-chain alkanes (propane and ethane), showing high productivity to olefins.

EXPERIMENTAL

Catalyst Preparation

A purely siliceous MCM-41 sample was prepared from a gel having the molar composition

$$SiO_2 : 0.12CTABr : 0.26TMAOH : 24H_2O,$$

were CTABr is cetyltrimethylammonium bromide (from Aldrich) and TMAOH is tetramethylammonium hydroxide (from Aldrich). The silica source was Aerosil-200 from Degussa. The crystallization was performed at 100°C for 48 h in Teflon-lined stainless steel autoclaves. The solid was recovered by filtration and exhaustive washing with distilled water until neutral pH in the filtrate was obtained. Then, the MCM-41 was dried at 60°C for 24 h. The occluded surfactant was removed by calcination at 540°C in nitrogen for 1 h and subsequently for 5 h in air, yielding the final mesoporous MCM-41 support.

MCM-supported vanadia catalysts were prepared by following a wet impregnation method. An ethanolic solution of vanadyl acetylacetonate to achieve a final V content of 0.6 to 10 wt% of V atoms was contacted with the MCM-41 carrier and the ethanol was rotaevaporated until complete dryness. The catalysts were heated overnight in air at 100°C and then calcined at 600°C for 6 h in air.

V-substituted mesoporous material (V–MCM-41) has been synthesized following a one-pot synthesis using $VOSO_4$ as the vanadium source. The gel, with the following molar composition

$$SiO_2 : 0.012VOSO_4 : 0.20CTAOH : 39H_2O,$$

was autoclaved in a Teflon-lined stainless steel reactor at 150°C for 24 h and then the resulting catalyst precursor was obtained after filtering, washing with distilled water, and drying at 60°C for 24 h (19). The sample was finally calcined at 600°C for 6 h.

The final V contents in the MCM's catalysts are summarized in Table 1. The impregnated samples have been named by a number, which indicates the V content in the calcined catalysts followed by MCM, which correspond to MCM-41. Thus, samples named as 2V/MCM is a supported catalyst with 2 wt% of V atoms. Vanadium-substituted mesoporous molecular sieve has been named as 0.6V–MCM-41.

TABLE 1

Characteristics of V-Containing MCM-41 Materials

Sample	V content		S_{BET}	θ	TPR results[c]	
	wt%[a]	mmol g^{-1}	(m^2 g^{-1})	(%)[b]	T_M (°C)	AOS
MCM-41	0.0	0	1050	0.0	—	—
0.6V/MCM	0.6	0.12	1013	0.7	480	4.5
2V/MCM	2.3	0.45	952	2.7	490	4.3
4V/MCM	4.2	0.80	833	5.1	496	4.1
7V/MCM	7.1	1.39	543	9.2	554	2.9
10V/MCM	10.3	2.02	50	14.3	Nd	Nd
0.6V–MCM	0.6	0.12	873	0.7	480	4.6

[a] Vanadium content, in wt% of V atoms, was determined by atomic absorption spectrometry.

[b] θ, theoretical vanadium superficial coverage (calculated for the unit area), have been obtained assuming the theroretical monolayer of vanadium to be 4.98×10^{18} molecules V_2O_5 cm^{-2} (1).

[c] Temperature of the maximum hydrogen consumption (T_M) and the average oxidation state (AOS) after reduction. Nd = not determined.

Catalyst Characterization

N_2 and Ar adsorption isotherms were determined in an ASAP 2010 instrument at 77 and 87 K, respectively, after the samples were degassed (1.33×10^{-2} Pa) at 400°C overnight.

X-ray diffraction patterns (XRD) were collected using a Philips X'Pert diffractometer equipped with a graphite monochromator, operating at 40 kV and 45 mA and employing nickel-filtered Cu$K\alpha$ radiation ($\lambda = 0.1542$ nm).

Diffuse reflectance UV–Vis spectra were collected on a Cary 5 equipped with a "Praying Mantis" attachment from Harric. The sample cell was equipped with a heater unit, a thermocouple, and a gas flow system for *in situ* measurements. The samples were dehydrated *in situ* in dry air at 400°C for 30 min. The spectra were recorded upon cooling down to room temperature, flowing dry air through the sample to avoid rehydration processes.

Prior to recording of the ^{51}V nuclear magnetic resonance (NMR) spectra, the samples were treated under dynamic vacuum at 373 K overnight and then transferred and sealed into the rotor in a glove box under an atmosphere of nitrogen. Solid state ^{51}V NMR spectra were recorded at ambient temperature on a Varian VXR-400S WB spectrometer at 105.1 MHz, using a high-speed MAS Doty probe with zircona rotors (5 mm in diameter). The spectra were acquired with pulses of 1 μs, corresponding to a flip angle of $\pi/13$, to avoid signal distortions of the $I = 7/2$ nuclei. The ^{51}V chemical shifts are referred against liquid $VOCl_3$ using a $Mg_3V_2O_8$ whose chemical shift is -554 ppm, as a secondary

reference. A solution of $NaVO_3$ was used to calibrate the radiofrequency power.

Temperature-programmed reduction (TPR) spectra were obtained on a 2910 Micromeritics apparatus loaded with 100 mg of catalyst. The samples were first treated in argon at room temperature for 1 h. The samples were subsequently contacted with an H_2/Ar mixture (H_2/Ar molar ratio of 0.15 and a total flow of 50 ml min^{-1}) and heated, at a rate of 10°C min^{-1}, to a final temperature of 1000°C.

Catalytic Tests

The catalytic experiments were carried out in a fixed bed quartz tubular reactor (i.d. 20 mm, length 400 mm), working at atmospheric pressure. The reactor was equipped with a coaxial thermocouple for catalytic bed temperature profiling (19). Catalyst samples (0.3- to 0.5-mm particle size) were introduced in the reactor and diluted with 8 g of silicon carbide (0.5- to 0.75-mm particle size) to keep a constant volume in the catalyst bed. The flow rate and the amount of catalyst were varied to different propane conversion levels. The feed consisted of a mixture of alkane/oxygen/helium with a molar ratio of 4/8/88. Experiments were carried out in the 500–550°C (propane) or 550–600°C (ethane) temperature interval to achieve the higher selectivity to partial oxidation products. Reactants and reaction products were analyzed by online gas chromatography, using two Hewlett-Packard apparatus equipped with three columns: (i) 23% SP-1700 Chromosorb PAW (30 m × $\frac{1}{8}$ in.) to separate hydrocarbons and CO_2; (ii) Carbosieve-S (8 m × $\frac{1}{8}$ in.) to separate O_2 and CO; (iii) Porapak Q (3.0 m × $\frac{1}{8}$ in.) to separate oxygenated products. Blank runs showed that under the experimental conditions used in this work the homogeneous reaction could be neglected.

RESULTS

Catalyst Characterization

MCM-41-supported vanadia samples (V loading from 0.6 to 7.0 wt%) present well-defined XRD patterns corresponding to MCM-41 structures (Fig. 1). It is notorious that the crystallinity of these V-containing materials decreases as the V loading increases, resulting in an amorphous solid when the V loading reaches a value close to 10 wt%, as deduced from the absence of low-angle reflections in the XRD pattern of the sample 10V/MCM.

The partial destruction of the mesoporous MCM-41 structure upon vanadium impregnation is further supported by the decrease of the surface area when the V content increases. Nevertheless, high surface areas (S_{BET}) (Table 1) and very narrow pore size distribution, calculated applying the Horwath–Kawazoe formalism to the Ar adsorption isotherms, are observed in MCM-41-supported materials with V loading lower than 7 wt%. From these results, it

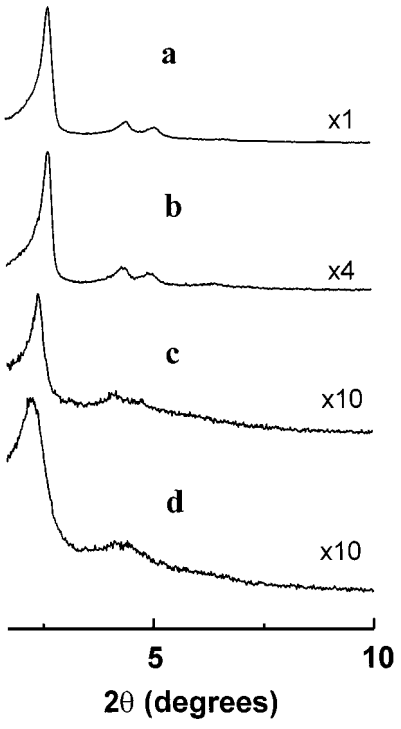

FIG. 1. X-ray diffraction patterns of calcined MCM-41-supported vanadia catalysts: (a) 0.6V/MCM; (b) 2V/MCM; (c) 4V/MCM; (d) 7V/MCM.

can be concluded that well-organized mesoporous catalysts were obtained upon V impregnation and subsequent calcination, being the maximum loading preserved the mesoporous structure close to 7 wt% of V atoms.

It is known that vanadium supported on siliceous materials can be easily hydrated, changing the nature of V species from tetracoordinated V to penta- or hexacoordinated sites (9, 19, 26, 27). For this reason, and in order to determine the exact vanadium environment, diffuse reflectance spectra in the UV–Vis region of MCM-41-supported samples were recorded in the dehydrated state. Figures 2 and 3 show the UV–Vis spectra of calcined VO$_x$/MCM samples after dehydration under dry air at 400°C (Fig. 2) and after rehydration at room temperature (Fig. 3). In the dehydrated form, the presence of a very broad band centered at ca. 300 nm is observed. This band can be deconvoluted in two main absorptions at 250 and 320 nm that are attributed to isolated V sites in tetrahedral coordination and to polymeric V−O−V species, respectively (19, 25–29). In addition, it can be seen that the center of the overlapping band shifts to higher wavelength when the V content increases as a consequence of the increase of the intensity of the absorption at 320 nm with respect to that appearing at 250 nm. Additionally, a new band at 450 nm appears for the solids with 7 wt% V loading assigned to the presence of V_2O_5 crystallites as a consequence of further polymerization of the V species (19, 25–29). The presence of these three bands has also been

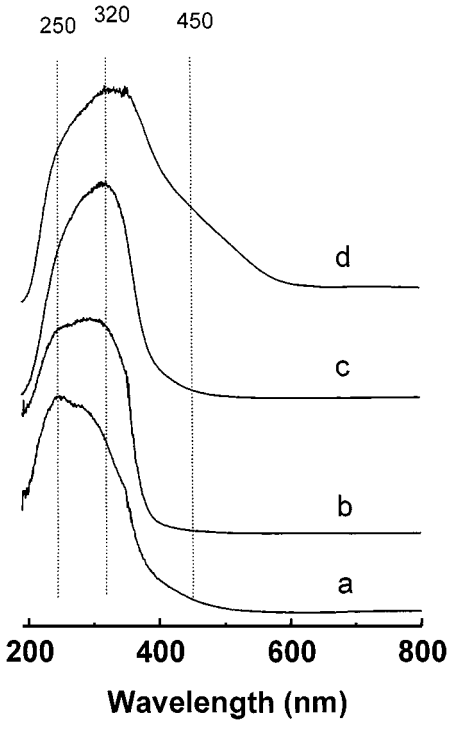

FIG. 2. Diffuse reflectance UV–Vis spectra of calcined MCM-41-supported vanadia catalysts after dehydration at 400°C, in air, for 1 h: (a) 0.6V/MCM; (b) 2V/MCM; (c) 4V/MCM; (d) 7V/MCM.

observed in silica-supported vanadia or V-substituted MCM-41 catalysts. (19, 25–29). Then, the observed increase of the relative intensities of the bands at 320 and 450 nm as the vanadium content increases can be explained as a consequence of the larger polymerization degree of vanadium species at high V loadings.

Additional information on the local coordination environment of V^{5+} cations has been obtained by solid state ^{51}V NMR spectroscopy. Although the ^{51}V nucleus possesses a quadrupolar spin ($I = 7/2$), which can lead to singularities in the NMR signals, it is usually admitted that the line shapes of the nonspinning spectra are dominated by the anisotropy of the chemical shift. This property has been taken as an advantage to extract information about the symmetry environment of vanadium sites in vanadium-containing catalysts by comparison with model compounds (30, 31). Figure 4 shows the ^{51}V wide-line NMR spectra of calcined 4V/MCM-41 and 7V/MCM-41 catalysts dehydrated and after hydration under ambient conditions. The NMR spectra of the dehydrated catalysts 4V/MCM (Fig. 4b) and 7V/MCM (Fig. 4d) consist of a resonance at −450 and −480 ppm, respectively, which can be attributed to distorted isolated tetrahedral V^{5+} of type $(SiO)_3{-}V{=}O$, in agreement with previous studies on VO_x/SiO_2 (30, 32) and V-containing mesoporous catalysts materials (25, 27). However, taking into consideration the UV–Vis results, we cannot rule out the contribution of low polymeric V^{5+} sites to the NMR signals of the dehydrated 4V/MCM-41 (Fig. 4b) and 7V/MCM-41 (Fig. 4d). A weak signal at −300 ppm appears in the spectrum of the dehydrated sample 7V/MCM-41 (Fig. 4d), which is typically ascribed to the perpendicular component $\delta_\perp$ of an axially symmetric signal of V^{5+} in a distorted octahedral or pseudo-octahedral symmetry as in V_2O_5, although the parallel component $\delta_{//} = -1270$ ppm is not detected in our spectrum (30, 31). The persistence of octahedral V^{5+} after dehydration must be due to the formation of a surface oxidic phase at higher vanadium content.

After hydration, two main signals, at −300 ppm and another one at ca. −580 and −540 ppm for 4V/MCM (Fig. 4a) and 7V/MCM (Fig. 4c), respectively, are evident in the NMR spectra. The resonance at −300 ppm can be ascribed to the perpendicular component $\delta_\perp$ of an axially symmetric signal of octahedral V^{5+} with the parallel part $\delta_{//}$, usually in the range between −900 and −1300 (30, 31), not distinguished in our spectra. The appearance of this signal after hydration indicates that a part of the tetrahedral vanadium coordinates to two (or one) extra water molecules to acquire octahedral (or pseudo-octahedral) coordination. This species would be of the $(SiO)_3{-}V{=}O(H_2O)_2$ type for isolated V^{5+} species. This observation is further supported by comparing the UV–Vis spectra of the hydrated 4V/MCM and 7V/MCM catalysts with those obtained in their rehydrated state (Fig. 3). There, it can be seen that

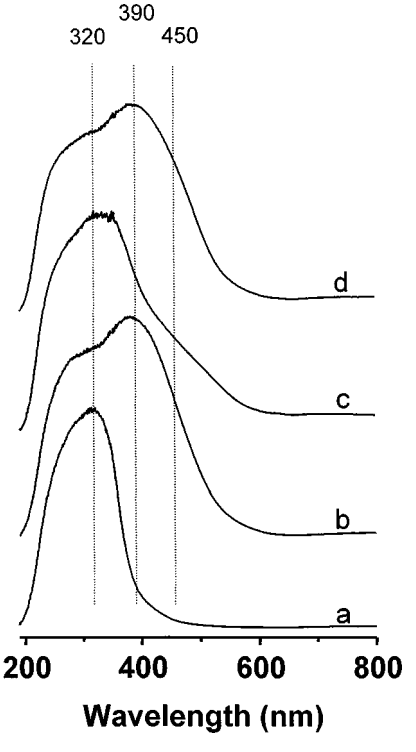

FIG. 3. Diffuse reflectance UV–Vis spectra of MCM-41-supported vanadia catalysts prior to and after hydration. (a) 4V/MCM-dehydrated; (b) 4V/MCM-hydrated; (c) 7V/MCM-dehydrated; (d) 7V/MCM-hydrated.

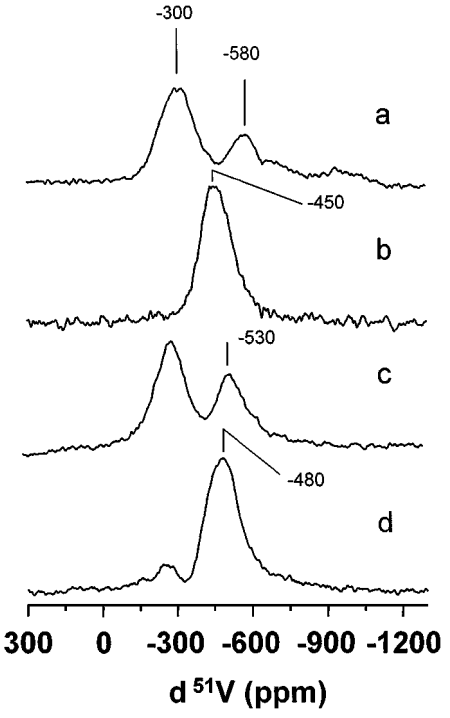

FIG. 4. ^{51}V wide-line NMR spectra of hydrated (a, c) and dehydrated (b, d) 4V/MCM (a, b) and 7V/MCM (c, d) catalysts.

upon hydration a new band at 390 nm appears which can be safely assigned to pseudo-octahedrically coordinated V^{5+} species as a consequence of the interaction of tetrahedral sites with two molecules of water. Interestingly, some of the V species remains in pure tetrahedral coordination, as can be deduced from the presence of the absorption at 320 nm in the UV–Vis spectra of the hydrated samples. This clearly indicates the existence of nonaccessible V species which can be ascribed to tetrahedral V sites buried within the pore walls of the siliceous MCM-41 structure.

The high-field resonance (at −530 or 580 ppm) possesses a low anisotropy of the chemical shift, typical for tetrahedral vanadium sites (30, 31), although it appears at a different position than that in the dehydrated catalysts. The fact that the some tetrahedral V^{5+} species do not increase their coordination has been previously attributed to their location in the pore walls, nonaccessible to water molecules (25), supporting our previous hypothesis. These species could also contribute to the high-field asymmetry of the NMR signals of the dehydrated catalysts (Figs. 4b and 4d).

The TPR patterns of V/MCM catalysts are comparatively shown in Fig. 5 and their main features summarized in Table 1. One peak at ca. 500°C is observed on MCM-supported samples with V loadings from 0.6 to 4 wt%. In the sample with high V content (7V/MCM) the main peak is shifted to 560°C and a shoulder appears at 590°C (Fig. 5d). The peak at low temperature should be related to the reduction of dispersed tetrahedral vanadium species, while the peak at 590°C should be related to the reduction of polymeric V^{5+} species V_2O_5-like (19, 21, 25, 26). The progressive shift of the maximum of the H_2 consumption peak to high temperature with the V loading could be related to a progressive formation of high polymeric vanadium species.

On the other hand, it can be observed in Table 1 that the average oxidation state (AOS) of vanadium in the reduced catalysts decreases as the V loading increases, and a sharp decrease of the AOS value from 4 to approximately 3 is observed for sample 7V/MCM. These results strongly suggest that "bulk-type" V_2O_5 could be reduced to a greater extent than isolated $(SiO)_3{\equiv}V{=}O$ sites.

Catalytic Tests in Oxidation Reactions

The catalytic results obtained in the oxidation of propane and ethane over V-containing MCM-41 are shown in Tables 2 and 3, respectively.

(a) Oxidative dehydrogenation of propane. Propylene, CO, and CO_2 were the main reaction products during the oxidation of propane on MCM-supported vanadia catalysts, although acetaldehyde and acrolein were also observed at high propane conversions and/or high reaction temperatures (Table 2). Since it is known that high selectivities to propylene are favored at high reaction temperatures on V-containing catalysts (1, 12), the propane oxidation has been mainly studied at 550°C.

Figure 6 shows that the selectivity to propylene decreases with the propane conversion on V/MCM catalysts. However, the catalytic behavior depends on the V content.

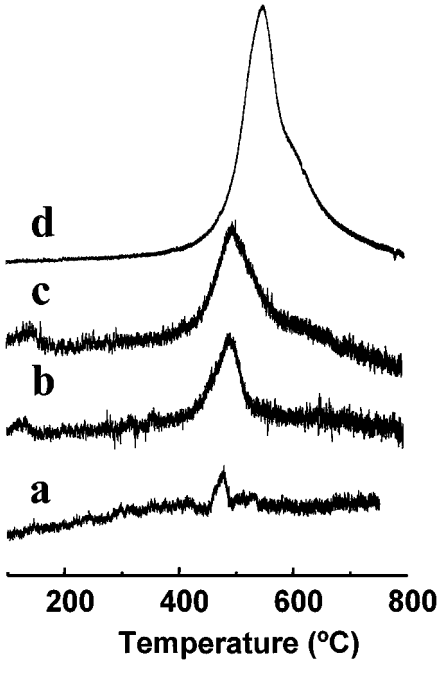

FIG. 5. TPR results of MCM-41-supported vanadium oxide catalysts: (a) 0.6V/MCM; (b) 2V/MCM; (c) 4V/MCM; (d) 7V/MCM.

TABLE 2

Oxidation of Propane on MCM-41-Supported Vanadia Catalysts at 550°C

Catalyst	W/F^a	C_3H_8 conv. (%)	Selectivity (%)				C_3H_6 yield (%)	STY_{C3H6} ($g\ kg_{cat}^{-1}\ h^{-1}$)[c]
			C_3H_6	Oxygenates[b]	CO	CO_2		
0.6V/MCM	26	14.8	60.9	8.1	17.7	12.3	9.0	145
2V/MCM	6	11.1	61.6	12.6	16.9	8.9	6.8	446
4V/MCM	6.5	16.3	51.6	9.0	27.6	11.8	5.5	550
7V/MCM	5	16.5	45.5	5.8	33.8	14.9	7.5	630
10V/MCM	5	16.1	42.7	5.2	35.8	16.3	6.9	580
0.6V–MCM	26	15.0	54.3	16.1	23.2	6.5	8.1	131

[a] Contact time, W/F, in g_{cat} h mol_{C3}^{-1}.
[b] Partial oxygenated products, i.e., acrolein and acetaldehyde.
[c] Rate of formation of propene per unit mass of catalyst per unit time, $STY_{C_3H_6}$ (space time yield) in $g_{C3H6}\ kg_{cat}^{-1}\ h^{-1}$, have been calculated at propane conversions of 15%.

Figure 7 compares the evolution of the selectivity to propylene at 550°C with the V loading (Fig. 7a) and the V surface density (Fig. 7b), at low and high propane conversions (15 and 40%, respectively). These results indicate that the selectivity to propylene on MCM-41-supported vanadia catalysts decreases when the V loading increases, although the selectivity to propylene reported here is higher than when SiO_2 is used as the support (19). However, the main difference between both supports is the higher vanadium surface density per gram of catalyst obtained on V/MCM catalysts due to the larger surface area of MCM-41 support.

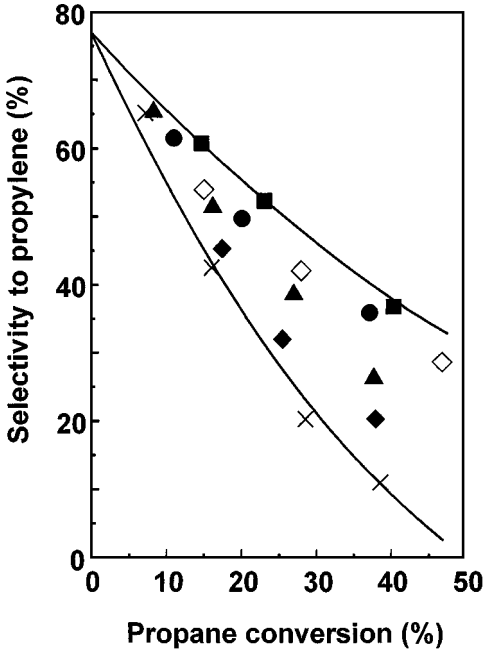

FIG. 6. Variation of the selectivity to propylene with the propane conversion obtained during the oxidation of propane at 550°C on vanadia supported on MCM-41. Catalysts: 0.6V/MCM (■); 2V/MCM (●); 4V/MCM (▲); 7V/MCM (◆); 10V/MCM (×); 0.6V–MCM-41 (◇).

The 0.6V–MCM-41 catalyst (prepared by hydrothermal synthesis) presents selectivity to propylene similar to that of the corresponding MCM-41-supported vanadia catalyst. However, the catalyst prepared by hydrothermal synthesis with high V loading presented selectivity to olefins lower than that on V/MCM-41 catalysts (19).

The formation rates of propylene per unit mass of catalyst per unit time, $STY_{C_3H_6}$, are comparatively shown in Table 2 and Fig. 7b. The V/MCM catalysts present a higher specific catalytic activity than V/SiO_2 catalysts (12), with formation rates of propylene over 700 $g_{C_3H_6}\ kg_{cat}\ h^{-1}$, keeping selectivities close to 50%. Moreover, MCM-41-supported vanadia catalysts present higher specific catalytic activity than V substituted MCM-41 materials, especially those with V contents higher than 1 wt% (19).

(b) Oxidative dehydrogenation of ethane. Ethylene, CO, and CO_2 were the main reaction products during the oxidation of ethane on MCM-supported vanadia catalysts, although acetaldehyde was also observed as a minor product (Table 3). It is known that high reaction temperatures favor higher selectivities to ethylene when the reaction is carried out on V-containing catalysts (1, 13). For this reason the reaction was mainly studied at 600°C.

Figure 8 shows the variation of the selectivity to ethylene with the ethane conversion obtained during the oxidation of ethane at 600°C on V-containing MCM-41 catalysts. The selectivity to ethylene decreases markedly as the ethane conversion increases, although this trend depends on the V content of the catalyst.

Figure 9 shows the variation of the selectivity to ethylene with the V loading (Fig. 9a) and the vanadium surface density of catalysts (Fig. 9b) at isoconversion conditions (conversion of ethane of 10 and 30%). It can be seen that the selectivity to ethylene depends strongly on the V loading but also on the ethane conversion. At low ethane conversions, the selectivity to ethylene increases initially with the V loading, presenting a maximum at about 2 wt%.

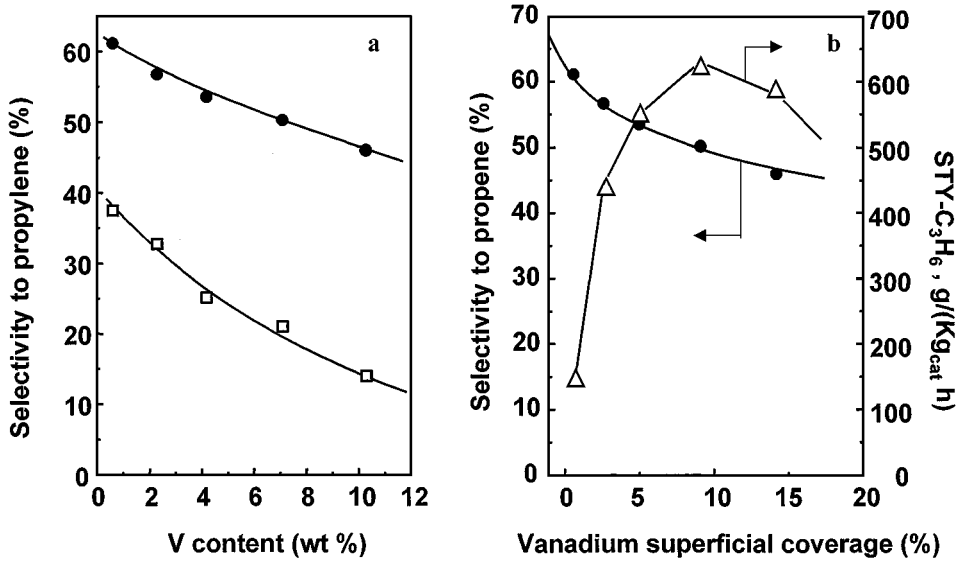

FIG. 7. Variation of the selectivity to propylene with the catalyst V content (a) or with the vanadium superficial coverage (b) and variation of the formation rate of propylene per unit mass of catalyst per unit time, $STY_{C_3H_6}$, with the vanadium superficial coverage (b) during the oxidation of propane at 550°C on V/MCM catalysts. Symbols: (●, □) selectivity to propylene at a propane conversion of 15 and 40% respectively; (△) formation rate of propylene per unit mass of catalyst per unit time, $STY_{C_3H_6}$.

However, at high ethane conversions, the selectivity to ethylene decreases when the V loading increases in the whole range of compositions.

When the variation of the selectivity to ethylene with the vanadium surface density is considered (Fig. 9b), it can be seen that catalysts with low vanadium surface density present lower initial selectivities to ethylene, which is further reduced at high ethane conversions.

Table 3 and Fig. 9b show the formation rates of ethylene per unit mass of catalyst per unit time, STY_{CH_2O}, obtained on V/MCM catalysts. The catalytic results presented here suggest that V/MCM catalysts present higher specific catalytic activities than V/SiO_2 catalysts (13), with formation rates of ethylene higher than 700 $g_{C_2H_4}$ kg_{cat} h^{-1} at selectivities to ethylene of 60%.

DISCUSSION

Previously reported results show that the incorporation of vanadium in MCM-41 materials by hydrothermal synthesis leads to low V contents (15–21) and that the selectivities to propylene decrease for V contents over 1 wt%. The amount of vanadium ions to be dispersed on MCM-41 can be increased by using conventional impregnation methods, as suggested from the characterization results presented here, and those previously reported on VO_x/MCM-41 (25) and VO_x/MCM-48 (26) supported vanadia catalysts. Since the nature of the vanadium species on MCM-41 obtained by both hydrothermal and impregnation methods appears to be the same, it is advantageous to use the latter since it allows dispersion of a higher amount of vanadium.

TABLE 3

Ethane Oxidation on MCM-41-Supported Vanadia Catalysts at 600°C

Catalyst	W/F[a]	C_2H_6 conv. (%)	Selectivity (%)[b]			C_2H_4 yield (%)	STY_{C2H4} (g kg_{cat}^{-1} h^{-1})[c]
			C_2H_4	CO	CO_2		
0.6V/MCM	38	13.0	58.8	26.3	15.0	7.6	56
2V/MCM	6.4	9.4	69.0	23.3	7.7	6.5	284
4V/MCM	3.2	8.4	68.6	21.9	9.5	5.8	508
7V/MCM	3.2	14.5	60.2	27.1	12.7	8.7	761
10V/MCM	22	28.2	38.3	52.0	9.7	10.8	137
0.6V–MCM	38	16.0	55.2	38.1	6.7	8.8	64.8

[a] Contact time, W/F, in g_{cat} h mol_{C2}^{-1}.
[b] Traces of acetaldehyde are also observed.
[c] Rate of formation of ethylene per unit mass of catalyst per unit time, STY_{C2H4} (space–time yield) in g_{C2H4} kg_{cat}^{-1} h^{-1}, have been calculated at ethane conversions of 15%.

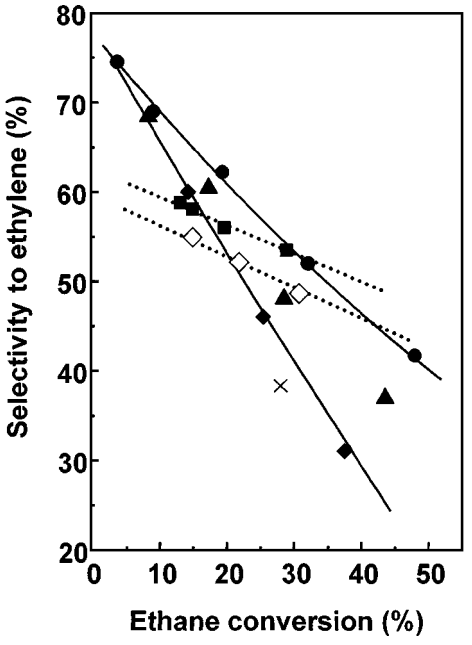

FIG. 8. Variation of the selectivity to ethylene with the ethane conversion obtained during the oxidation of ethane at 600°C on vanadia supported on MCM-41. Symbols as in Fig. 6.

The application of UV–Vis diffuse reflectance spectroscopy to characterize the dehydrated vanadia-supported MCM-41 catalysts shows that, at low V content, isolated tetrahedral V^{5+} species of type $(SiO)_3{\equiv}V{=}O$ are predominant. At higher V loading, low polymeric V^{5+}species become more abundant, and at 7 wt%, octahedral V^{5+} forming the oxide phase is also present. The ^{51}V NMR results of the dehydrated 4V/MCM-41 and 7V/MCM-41 catalysts confirm that most vanadium cations are tetrahedrally coordinated and that a V_2O_5-like phase begins to appear in the 7V/MCM sample. The ^{51}V MAS NMR and UV–vis spectra of the samples recorded under ambient conditions show that most vanadiums are able to coordinate additional water molecules and therefore are located in accessible sites. The vanadium species remaining in tetrahedral coordination in the presence of moisture has been attributed to nonaccessible V^{5+} buried in the pore walls. Similar UV–Vis and ^{51}V MAS NMR spectra have been reported previously in V-substituted MCM-41 (15–21) but also on SiO_2-supported vanadia (10–13) or V silicalite (6, 7, 9, 33). Therefore, the vanadium species formed on siliceous or mesoporous MCM-41 supports must be similar.

The TPR results show that the reducibility of the isolated V^{5+} species, which are predominant at low V contents, is similar to that reported for this species on SiO_2 (7–13). Polymeric V^{5+} species and/or V_2O_5 crystallites, formed on catalysts with V loading higher than 4 wt% (VO_x/MCM-41), are more difficult to reduce. Again, the reducibility behavior of vanadia supported on mesoporous MCM-41 suggests that the same types of vanadium species observed on V/SiO_2 catalysts are formed on MCM-41 support.

In agreement with the catalytic results obtained during the oxidation of propane and ethane, the following reaction

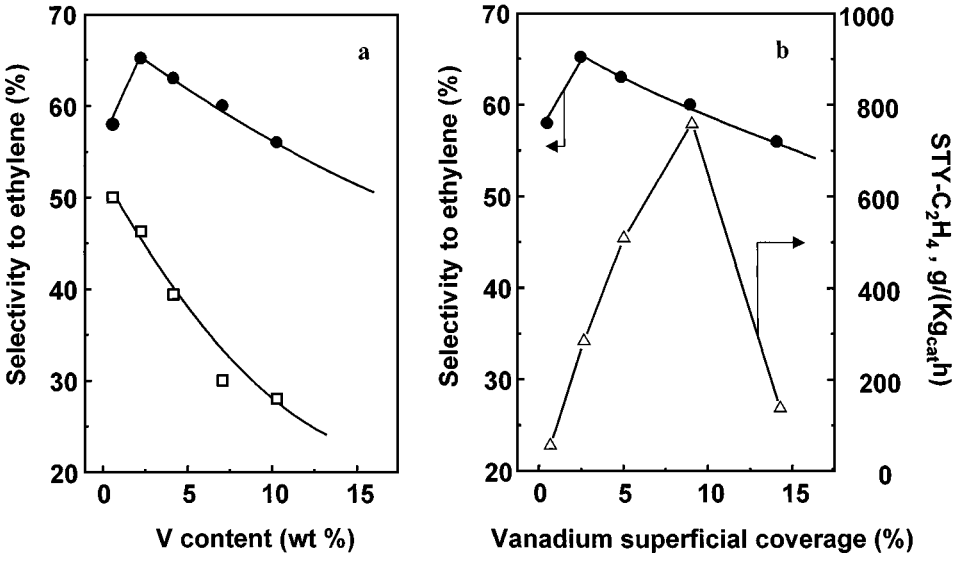

FIG. 9. Variation of the selectivity to ethylene with the catalyst V content (a) or with the vanadium superficial coverage (b) of catalyst and variation in the formation rate of ethylene per unit mass of catalyst per unit time, $STY_{C_2H_4}$, with the vanadium superficial coverage (b) of catalyst obtained during the oxidation of ethane at 600°C on V/MCM catalysts. Symbols: (●, □) selectivity to ethylene at a ethane conversion of 15 and 40%, respectively; (△) formation rate of ethylene per unit mass of catalyst per unit time, $STY_{C_2H_4}$.

network can be proposed:

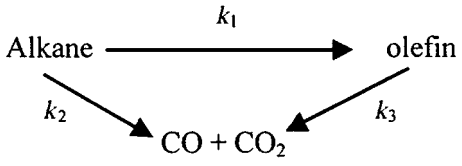

Propylene or ethylene are the most abundant primary products during the oxidation of propane or ethane, respectively, while CO and CO_2 comes from the deep oxidation of both the alkane and the corresponding olefin. This reaction network has also been reported on previous supported vanadia catalysts (1, 19, 28, 29, 34, 35).

The high selectivities to oxydehydrogenation products obtained on MCM-supported catalysts are a consequence of the high dispersion of vanadium and the lower formation of V_2O_5 crystallites. This permits the increase of the V loading, keeping high selectivities to olefins (Tables 2 and 3), therefore yielding a higher productivity to olefins with respect to V-substituted MCM-41 (19, 21) or V/SiO_2 (12, 13) catalysts.

Interesting differences in the evolution of the selectivities to olefin with the V loading at low and high alkane conversions are also observed (Figs. 7 and 9). As suggested in the oxidative dehydrogenation of propane (1, 19, 28, 34), the selectivity to olefin at low alkane conversion is related to the k_1/k_3 ratio, whereas at high alkane conversion, it is related to the $k_1/(k_2 + k_3)$ ratio.

Catalysts with high V loading give better selectivity to olefins at low alkane conversions because of the selective alkane activation. However, the selectivity to olefin is lowered, at high alkane conversions, as a consequence of their activity in the conversion of the corresponding olefin.

In contrast, catalysts with low V loading present low initial selectivity to olefins, but they also give low activity in the combustion of ethylene. These results suggest that the number of active and nonselective sites for the production of olefins decrease after the incorporation of V atoms, which could explain the initial better selectivity on catalysts with high V loading. So V sites are the active and selective sites in the OXDH of propane and ethane, although the agregation of V atoms can modify the catalytic behavior.

The strong influence of the reaction temperature on the catalytic behavior of supported vanadium oxide catalysts has been related to the reducibility of the active sites (V atoms) and the reactivity of the alkane fed (1, 35–37). The reactivity of propane is about 4 times higher than that of ethane, and then our results suggest that the lower the reactivity of the hydrocarbon fed, the higher the influence of the V loading on the selectivity to partial oxidation products.

Table 4 shows the activity of MCM-41-supported vanadia catalysts for the OXDH of propane and ethane. In the case of propane, the TOF decreases with the V loading, i.e., as the presence of V_2O_5 crystallites increases. However, similar TOF were obtained during the OXDH of ethane on catalysts with V contents of 0.6–7 wt%.

TABLE 4

OXDH Activity of MCM-41-Supported Vanadia Catalysts for Propane and Ethane Oxidation at 550°C

Catalyst	Propane OXDH TOF (s^{-1})[a]	Ethane OXDH TOF (s^{-1})[a]
0.6V/MCM	6.8×10^{-3}	1.2×10^{-3}
2V/MCM	6.6×10^{-3}	1.1×10^{-3}
4V/MCM	5.1×10^{-3}	1.2×10^{-3}
7V/MCM	3.9×10^{-3}	1.2×10^{-3}
10V/MCM	0.6×10^{-3}	0.2×10^{-3}

[a] TOF is calculated at alkane conversions lower than 5%, considering the amount of olefin (propylene or ethylene) formed, and on the basis of the total V atoms in the catalyst.

Isolated tetrahedral V^{5+} species appear to be the selective sites in the oxidative dehydrogenation of propane, as has previously been proposed in V–MCM-41 (19–21), V-containing microporous materials (5–8), or supported vanadia (1, 9–13) catalysts. The polymerization degree of the surface vanadia species and the appearance of V_2O_5 crystallites have a significant effect on the selectivity to propylene. As has been suggested, the surface propyl species or adsorbed propylene may react over two V atoms of V−O−V or

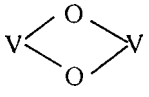

pairs (38, 39) favoring the consecutive reactions and decreasing the selectivity to propylene from propane.

In contrast, the polymerization degree of the surface vanadia species and the appearance of V_2O_5 crystallites have a smaller influence on the selectivity to ethylene during the OXDH of ethane, as suggested by SiO_2-supported vanadia catalysts (40). In this case, an interaction between ethyl species with two V atoms of V−O−V pairs is not expected as a consequence of the short distance between the two terminal carbon atoms (39). So, in the case of the OXDH of ethane, a low negative effect of the presence of V−O−V pairs in the catalyst on the selectivity to oxydehydrogenation products is expected. This is in agreement with the catalytic results reported during the ethane oxidation on $(VO)_2P_2O_7$ (39).

In conclusion, MCM-41-supported vanadia catalysts are active and selective in the oxidative dehydrogenation of ethane and propane. They present the same V^{5+} species as those reported in V-substituted MCM-41 (prepared hydrothermally), V silicalite, or SiO_2-supported vanadia catalysts. Their catalytic properties and the amount of V atoms dispersed on the surface of MCM-41 are related to both the

high surface area and the number of hydroxyl groups of the oxide support. In this way, high productivities keeping high selectivities to olefins can be achieved during the oxidative dehydrogenation of propane and ethane.

ACKNOWLEDGMENTS

Financial support from DGICYT, Spain (Projects PPQ2000-1396 and MAT 2000-1167-CO2-01), is gratefully acknowledged. M.L.P. and B.S. are thankful for a postgraduate scholarship to the Ministerio de Educación y Cultura and to the Conselleria de Cultura, Educació i Ciència, respectively.

REFERENCES

1. Blasco, T., and López Nieto, J. M., *Appl. Catal. A* **157**, 117 (1997).
2. Centi, G., *Appl. Catal. A* **147**, 267 (1996).
3. Deo, G., Wachs I. E., and Haber, J., *Crit. Rev. Surf. Chem*. **4**, 141 (1994).
4. Bond, G. C., and Tahir, S. F., *Appl. Catal.* **71**, 1 (1991).
5. López Nieto, J. M., *Top. Catal.* **15**, 189 (2001).
6. Zatorski, L. W., Centi, G., López Nieto, J. M., Trifiró, F., Bellusi G., and Fattore, V., *Stud. Surf. Sci. Catal.* **49**, 1243 (1989).
7. Centi G., and Trifiró, F., *Appl. Catal. A* **143**, 3 (1996).
8. Blasco, T., Concepción, P., López Nieto J. M., and Pérez-Pariente, J., *J. Catal.* **152**, 1 (1995).
9. Wang, Ch.B., Deo, G., and Wachs, I. E., *J. Catal.* **178**, 640 (1998).
10. Bañares, M., Cao, X., Fierro J. L. G., and Wachs, I. E., *Stud. Surf. Sci. Catal.* **110**, 295 (1997).
11. Owens L., and Kung, H. H., *J. Catal.* **144**, 202 (1993).
12. Puglisi, M., Arena, F., Frusteri, F., Sokolovskii, V., and Parmaliana, A., *Catal. Lett.* **41**, 41 (1996).
13. Le Bars, J., Vedrine, J. C., Auroux, A., Trautman, S., and Baerns, M., *Appl. Catal. A* **88**, 179 (1992) .
14. Beck, J. S., U.S. Patent 5,057,296 (1991).
15. Neumann, R., and Khenkin, A. M., *Chem. Commun.* 2643 (1996). Sayari, A., *Chem. Mater.* **8**, 1840 (1996).
16. Gontier S., and Tuel, A., *Microporous Mater.* **5**, 161 (1995).
17. Centi, G., Fazzani, F., Canesson, L., and Tuel, A., *Stud. Surf. Sci. Catal.* **110**, 893 (1997).
18. Lim, S., and Haller, G. L., *Appl. Catal. A* **188**, 277 (1999).
19. Peña, M. L., Dejoz, A., Fornés, V., Rey, F., Vázquez, M. I., and López Nieto, J. M., *Appl. Catal. A* **209**, 155 (2001).
20. López Nieto, J. M., Peña, M. L., Rey, F., Dejoz, A., and Vázquez, M. I., *in* "Abstract of 217th ACS National Meeting, Anaheim, 1999," CATL-012. *Am. Chem. Soc.*, Washington, D.C., 1999.
21. Santamaria-González, J., Luque-Zambrana, J., Mérida-Robles, J., Maireles-Torres, P., Rodríguez-Castellón, E., and Jiménez-López, A., *Catal. Lett.* **68**, 67 (2000).
22. Grubert, G., Rathouski, J., Schulz-Ekloff, G., Wark, M., and Zukal, A., *Microporous Mesoporous Mater.* **22**, 225 (1998).
23. Wan, Z., and Kevan, L., *J. Phys. Chem. B* **101**, 2020 (1997).
24. Newman, R., and Levin-Elad, M., *Appl. Catal. A* **122**, 85 (1995).
25. Berndt, H., Martin, A., Brückner, A., Schreier, E., Muller, D., Kosslick, H., Wolf G. V., and Lücke, B., *J. Catal.* **191**, 284 (2000).
26. Baltes, M., Cassiers, K., Van der Voort, P., Weckhuysen, B. M., Schoonheydt, R. A., and Vansant, E. F., *J. Catal.* **197**, 160 (2001).
27. Wei, D., Wang, H., Feng, X., Chueh, W.-T., Ravikovitch, P., Lyubovsky, M., Li, C., Takeguchi, T., and Haller, G. L., *J. Phys. Chem. B* **103**, 2113 (1999).
28. Chen, K., Iglesia, E., and Bell, A. T., *J. Catal.* **192**, 197 (2000).
29. Male, J. L., Niessen, H. G., Bell, A. T., and Tilley, T. D., *J. Catal.* **194**, 431 (2000).
30. Lapina, O. B., Mastikhin, V. M., Shubin, A. A., Krasilnikov, V. N., and Zamarev, K. I., *Prog. Nucl. Magn. Reson. Spectrosc.* **24**, 457 (1992).
31. Eckert, H., and Wachs, I. E., *J. Phys. Chem*. **93**, 6796 (1989).
32. Das, N., Eckert, H., Hu, H., Wachs, I. E., Walzer, J. F., and Feher, F. J., *J. Phys. Chem*. **97**, 8240 (1993).
33. Centi, G., Perhatoner, S., Trifiró, F., Aboukais, A., Aissi, C. F., and Guelton, M., *J. Phys. Chem*. **96**, 2617 (1992).
34. Concepción, P., López Nieto, J. M., and Pérez-Pariente, J., *J. Mol. Catal. A* **99**, 173 (1995).
35. López Nieto, J. M., Soler, J., Concepción, P., Herguido, J., Menéndez, M., and Santamaria, J., *J. Catal.* **185**, 324 (1999).
36. Lemonidou, A. A., Tjatjopoulos, G. J., and Vasalos, I. A., *Catal. Today* **45**, 65 (1998).
37. Pacheco, M. L., Soler, J., Dejoz, A., López Nieto, J. M., Herguido, J., Menéndez, M., and Santamaria, J., *Catal. Today* **61**, 101 (2000).
38. Corma, A., López Nieto, J. M., Paredes, N., Perez, M., Shen, Y., Cao, H., and Suib, S. L., *Stud. Surf. Sci. Catal.* **72**, 213 (1992).
39. Michalakos, P. M., Kung, M. C., and Kung, H. H., *J. Catal.* **140**, 226 (1993).
40. Gao, X., Bañares, M. A., and Wachs, I. E., *J. Catal.* **188**, 325 (1999).